

# Data Arrangement With Rotation Transformation for Fully Polarimetric Synthetic Aperture Radar

著者(英)	Fang Shang, Xiaoyun Huang, Hai Liu, Akira Hirose
journal or publication title	IEEE Geoscience and Remote Sensing Letters
page range	1-5
year	2019-07-04
URL	<a href="http://id.nii.ac.jp/1438/00009307/">http://id.nii.ac.jp/1438/00009307/</a>

doi: 10.1109/LGRS.2019.2924077

# Data Arrangement with Rotation Transformation for Fully Polarimetric Synthetic Aperture Radar

Fang Shang, *Member, IEEE*, Xiaoyun Huang, *Member, IEEE*, Hai Liu, *Member, IEEE*, Akira Hirose, *Fellow, IEEE*

**Abstract**—This paper proposes a data arrangement for fully polarimetric synthetic aperture radar (SAR). It is an essentially novel method in the use of the rotation transformation in data interpretation. The key point of the proposal is employing single pixel based and selective rotation transformation for each pixel before the speckle filtering. The experimental results with ALOS2-PALSAR2 data show that the proposed data arrangement has much higher performance in recognizing double bounce scattering in man-made target area. At the same time, it is effective in avoiding the overestimation of double bounce and/or surface scattering in natural target areas.

## I. INTRODUCTION

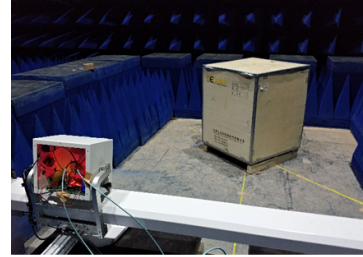
Polarimetric synthetic aperture radar (PolSAR) system is highly expected in land target observation [1]–[5]. The scattering model based decompositions are widely used for interpreting the scattering mechanisms [3]–[5]. In such methods, the models are defined in their standard local coordinate systems. In practical observation, there is usually a rotation shift in the measured data from the standard formation. In order to improve the interpreting performance, the rotation transformations are introduced to the decompositions [5]–[7]. It has been proved in many cases that the decompositions with the rotation transformations achieve much better results. However, there are some aspects needed to be discussed further. Firstly, many works were trying to rigorously relate the shift angle with the orientation angle of the targets [5], [8]. However, when the targets cannot provide directly back-forward reflection, it is hard to find a pure relationship between the rotation angle of the data and the geometrical orientation angle of the targets. Secondly, the rotation transformations are usually implemented on the averaged coherency matrix. Such a process is equivalent to applying the same rotation angle to all the pixels in a local window. Only a part of the data in the window can be rotated to fit the standard coordinate systems appropriately. Thirdly, in most works, the rotation transformation is implemented for all the pixels. However, the rotation transformation is not always rational. It may cause an overestimation of double bounce and/or surface scattering in natural target areas.

Fang Shang is with the Department of Computer and Network Engineering, University of Electro-Communications, 1-5-1 Chofugaoka, Chofu, Tokyo 182-0021, Japan. e-mail: shangfang@uec.ac.jp

Xiaoyun Huang is with the Institute of Electromagnetics and Acoustics, Xiamen University, Xiamen 361008, China

Hai Liu is with the School of Civil Engineering, Guangzhou University, Guangzhou 510006, China. e-mail: hliu@gzhu.edu.cn

Akira Hirose is with the Department of Electrical Engineering and Information Systems, The Tokyo University, 7-3-1 Hongo, Bunkyo-ku, Tokyo 113-8656, Japan. e-mail: ahirose@ee.t.u-tokyo.ac.jp



Center frequency 3.025 GHz  
Bandwidth: 3 GHz  
Orbit distance : 1400 mm  
Orbit length : 1200 mm  
Scanning step: 10 mm  
Off-nadir angle: 30°  
Target: 0.5 m × 0.5 m × 0.5 m

Calculated Rotation Angle of the Experimental Data

Target Orientation angle	10°	30°	50°	70°
Calculated Rotation Angle	-4.6°	-12.8°	-7.9°	-7.6°

Fig. 1. Experiment for testing the relationship between the calculated rotation angle and the target orientation angle.

In this paper, considering the aspects above, we propose a data arrangement for fully polarimetric SAR. It is an essentially novel method in the use of the rotation transformation in data interpretation. The key point of the proposed algorithm is to employ single pixel based and selective rotation transformation applied to each pixel before the speckle filtering. In section II, problems in recent decompositions are discussed. In section III, the proposed data arrangement is described. In section IV, the performance is evaluated with ALOS2-PALSAR2 data for Ebetsu city area, Japan.

## II. DISCUSSION ON ROTATION TRANSFORMATION IN RECENT DECOMPOSITIONS

There are three aspects need to be discussed for the conventional rotation transformations.

### A. Explanation of Rotation Angle

In many works the geometrical meaning of the rotation angle is explained as coinciding [5], or rigorously relating [8] with the orientation angle of the targets. However, when the target is not facing to the radar, the dominant power of the reflected wave cannot get back to the radar. In such a case, factors such as material feature, surface roughness, and detail structures on the facade may also cause obvious additional rotation shift in the scattered wave. The orientation angle of the targets is not the unique and/or dominant factor having influence on the angle shift of the data. Therefore, the calculated rotation angle is not purely or rigorously related to the target orientation direction angle. We designed scaling experiments in laboratory to test the relationship between the calculated rotation angle and the orientation direction angle as shown in Fig. 1. The results summarized below the figure show

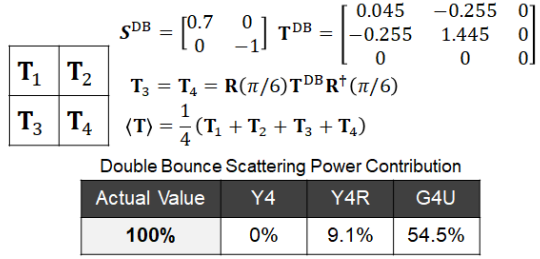


Fig. 2. Example for testing the capability for improving double bounce scattering power contribution.

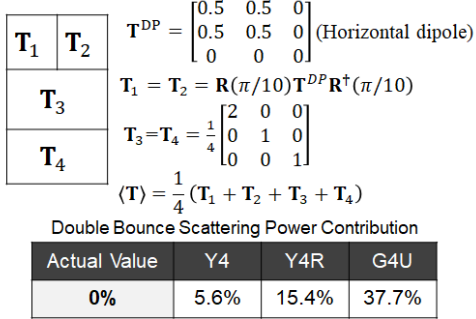


Fig. 3. Example for testing the rationality of rotation transformation.

that the calculated rotation angels are not obviously related with the actual target orientation angles. The explanation needs to be reconsidered.

### B. Capability of Improving Double Bounce Scattering Power Contribution

The main advantage of the rotation transformation is that the double bounce scattering power contribution can be improved for the man-made targets to approach the actual value [5], [6]. However, there is a theoretical limitation. For instance, consider the window shown in Fig. 2. In each pixel, the measured  $\mathbf{T}$  matrix  $\mathbf{T}_i$  is a double bounce model. Here,  $\mathbf{T}_3$  and  $\mathbf{T}_4$  have a  $\pi/6$  coordinate rotation. The rotation matrix is defined as

$$\mathbf{R}(\theta) = \begin{bmatrix} 1 & 0 & 0 \\ 0 & \cos 2\theta & \sin 2\theta \\ 0 & -\sin 2\theta & \cos 2\theta \end{bmatrix} \quad (1)$$

In this case, the double bounce scattering power contribution is actually 100%. The interpretation results of Y4, Y4R, and G4U methods for this window are shown in Fig. 2. Both of the Y4R and the G4U methods can improve the double bounce scattering. However, the improved contributions are still far from the actual value (100%). The reason is that, such a process is equivalent to implement the same rotation angle to all the pixels. Only the data of part of the pixels can be rotated to fit the standard double bounce scattering model. If we use “single pixel based rotation transformation”, it is possible to overcome the limitation.

### C. Rationality of Rotation Transformation

The rotation transformation is usually implemented for all the pixels. However, for some targets, the transformation is not rational enough. Take the window shown in Fig. 3 as an example. This window includes two pixels with the same  $\pi/10$  dipole model and two small areas with the uniform distribution volume scattering model. In this window, the actual double bounce scattering is 0%. The double bounce scattering power contribution calculated by the Y4, Y4R, and G4U methods for this window are shown in Fig. 3. Here, the performance of the decomposition without rotation transformation is better in this case. This example indicates that the rotation transformation is not always rational. For a certain pixel, if we have a judgment on the rationality and necessity before implementing a rotation transformation, the decomposition performance can be possibly improved.

## III. DATA ARRANGEMENT WITH ROTATION TRANSFORMATION

Considering the aspects discussed in Section II, we propose a data arrangement for fully polarimetric SAR employing single pixel based and selective rotation transformation before the speckle filtering.

### A. Single Pixel Based Rotation Transformation

In this paper, the rotation transformation is implemented to the measured scattering matrix of each pixel to estimate the rotation angle of the local coordinate-system. Before the rotation transformation, calibrations such as absolute radiometric calibration, Faraday compensation, and symmetry calibration should be done. The scattering matrix after calibration is written as

$$\mathbf{S}^c = \begin{bmatrix} S_{hh}^c & S_{hv}^c \\ S_{vh}^c & S_{vv}^c \end{bmatrix} \quad (2)$$

Here,  $S_{hv}^c = S_{vh}^c$ . The rotation transformation for the scattering matrix is

$$\mathbf{S}^c(\theta) = \begin{bmatrix} S_{hh}^c(\theta) & S_{hv}^c(\theta) \\ S_{vh}^c(\theta) & S_{vv}^c(\theta) \end{bmatrix} = \mathbf{R}_s(\theta) \mathbf{S}^c \mathbf{R}_s(\theta)^\dagger \quad (3)$$

where the rotation matrix  $\mathbf{R}_s$  is defined as

$$\mathbf{R}_s(\theta) = \begin{bmatrix} \cos \theta & \sin \theta \\ -\sin \theta & \cos \theta \end{bmatrix} \quad (4)$$

In a standard coordinate-system, the off-diagonal elements of the scattering matrix has minimum power in comparison with that in other coordinates. Therefore, the angle  $\theta$  is selected to force the  $|S_{hv}^c(\theta)|^2$  to be lowest. According to (3), the power of the  $S_{hv}^c$  elements can be described as

$$|S_{hv}^c(\theta)|^2 = \frac{1}{2} (|B|^2 + |A|^2) + \sqrt{P^2 + Q^2} \sin(4\theta + \psi) \quad (5)$$

where  $A = \frac{1}{2}(S_{vv}^c - S_{hh}^c)$ ,  $B = S_{hv}^c$ ,  $P = \frac{1}{2}(|B|^2 - |A|^2)$ , and  $Q = \text{Re}\{AB^*\}$ . The angle  $\psi \in [0, 2\pi]$  is determined by

$$\psi = \begin{cases} \arccos\left(\frac{Q}{\sqrt{P^2+Q^2}}\right) & \text{if } P \geq 0 \\ 2\pi - \arccos\left(\frac{Q}{\sqrt{P^2+Q^2}}\right) & \text{if } P < 0 \end{cases} \quad (6)$$

Here,  $\arccos(\cdot) \in [0, \pi]$ . Subsequently, the minimum value of  $|S_{hv}^c(\theta)|^2$  is achieved when  $\sin(4\theta + \psi) = -1$ . There are infinite solutions of angle  $\theta$  with period  $\frac{\pi}{2}$ . We can note all the solutions as  $\theta = \{\frac{3\pi}{8} - \frac{1}{4}\psi + \frac{n\pi}{2}\}$  where  $n$  can be any integer. The solution with the smallest absolute value  $\theta_0$  is selected as the calculated rotation angle.

$$\theta_0 = \arg \min_{\theta} \left\{ |\theta| \mid \theta = \frac{3\pi}{8} - \frac{1}{4}\psi + \frac{n\pi}{2}, n \in \mathcal{Z} \right\} \quad (7)$$

The value range of  $\theta_0$  is  $\theta_0 \in (-\frac{\pi}{4}, \frac{\pi}{4})$ .

### B. Data Arrangement

The rotation angle  $\theta_0$  is calculated for each pixel in an observation area. Next, for each certain pixel, we need to judge whether the pixel need to be arranged with rotation transformation or not. A basic requirement of the arrangement is that the configuration characteristics of targets should be protected. For the targets with obviously orientated configurations, such as farmlands and cities, the rotation transformation can improve their recognizability in the following scattering mechanism interpretation, whereas, for targets with many randomly orientated configurations such as forests, the rotation transformation will destroy the randomness and cause surface and/or double bounce reflection scattering to be overestimated. Here, we propose a parameter named ‘‘bias degree’’ to evaluate the characteristics. The bias degree for pixel  $[I]$  is defined as

$$D_b^{[I]} = \frac{1}{N \times N} \sum_{\theta_0^w \in W_{N \times N}^{[I]}} \text{sgn}(\theta_0^w) \quad (8)$$

where  $[I]$  is the index of the pixel,  $W_{N \times N}^{[I]}$  denotes an  $N \times N$  pixels window centered at pixel  $[I]$ ,  $\theta_0^w$  is the calculated rotation of a pixel in window  $W_{N \times N}^{[I]}$ , and  $\text{sgn}(\cdot)$  denotes the sign function. The sign of  $\theta_0$  is related with the rotation direction. Therefore, the parameter  $D_b^{[m,n]}$  roughly expresses the  $\theta_0$  distributing situation in the window  $W_{N \times N}^{[I]}$ . If the distribution is almost random, the  $D_b^{[I]}$  will be closed to 0. The condition for considering a pixel as having obvious bias is

$$|D_b^{[I]}| > \delta_b \quad (9)$$

where  $\delta_b \in (0, 1)$  is the threshold for judging the bias level. If (9) is satisfied, the rotation transformation is basically rational for pixel  $[I]$ . We should note that when the distributing center is closed to 0 and the number of pixels distributing near the center is high, the bias degree can be also obvious. However, in this case, most of the calculated rotation angles are very small which may be caused by measuring errors. The targets with randomly orientated configurations also possibly lead to such a distribution. Therefore, we name the high bias in this

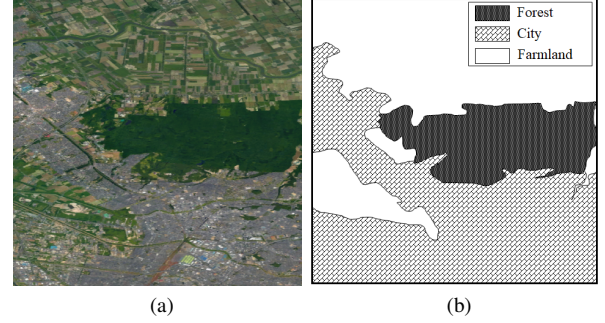


Fig. 4. (a) Google satellite photo of Ebetsu area, and (b) the sketch of the photo.

case a ‘‘pseudo-bias’’. A pixel with pseudo-bias should not be implemented rotation transformation.

In order to eliminate pixels with pseudo-bias, the probability density function (PDF) of  $\theta_0$  distribution in the  $W_{N \times N}^{[I]}$  window, written as  $f^{[I]}(\theta)$ , is estimated for the pixels with obvious  $\theta_0$  bias. The  $f^{[I]}(\theta)$  is defined as

$$f^{[I]}(\theta) = \frac{g^{[I]}(\theta)}{\int_{-\frac{\pi}{4}}^{\frac{\pi}{4}} g^{[I]}(\theta)} \quad (10)$$

where

$$g^{[I]}(\theta) = \sum_{\theta_0^w \in W_{N \times N}^{[I]}} \frac{1}{\sigma_g \sqrt{2\pi}} e^{-\frac{(\theta - \theta_0^w)^2}{2\sigma_g^2}} \quad (11)$$

Here, the measured rotation angle  $\theta_0^w$  for each certain pixel in the window is statistically expressed by a Gaussian distribution with the mean  $\theta_0^w$  and the standard deviation  $\sigma_g$ . By summing functions of all the pixels in the window, as shown in equation (11), we can have continuous probability density function (PDF) for the window. A similar probability density function estimation is mentioned in [10]. Two parameters are used to describe the feature of the PDF, i.e., the distributing center  $\mu^{[I]}$ , and the maximal density  $\Phi^{[I]}$ .

$$\begin{aligned} \mu^{[I]} &= \arg \max_{\theta \in [-\frac{\pi}{4}, \frac{\pi}{4}]} \left\{ f^{[I]}(\theta) \right\} \\ \Phi^{[I]} &= f(\mu^{[I]}) \end{aligned} \quad (12)$$

The conditions for treating a pixel as having pseudo-bias is

$$|\mu^{[I]} - \mu_0| < \delta_\mu \quad \text{and} \quad \frac{|\Phi^{[I]} - \Phi_0|}{\Phi_0} < \delta_\Phi \quad (13)$$

where  $\delta_\mu \in (0, \frac{\pi}{4})$  and  $\delta_\Phi \in (0, 1)$ . The  $\mu_0$  and  $\Phi_0$  are the distributing center and the maximal density of a reference PDF, If (13) is satisfied, the pixel will keep still without rotation transformation. Otherwise, we implement the rotation transformation.

### C. Summary of the Procedures

The procedures of the proposed data arrangement are summarized as follows.

STEP 1 Calculate the single pixel based rotation angles  $\theta_0$  for all the pixels in the observed area using equation (2) to (7).

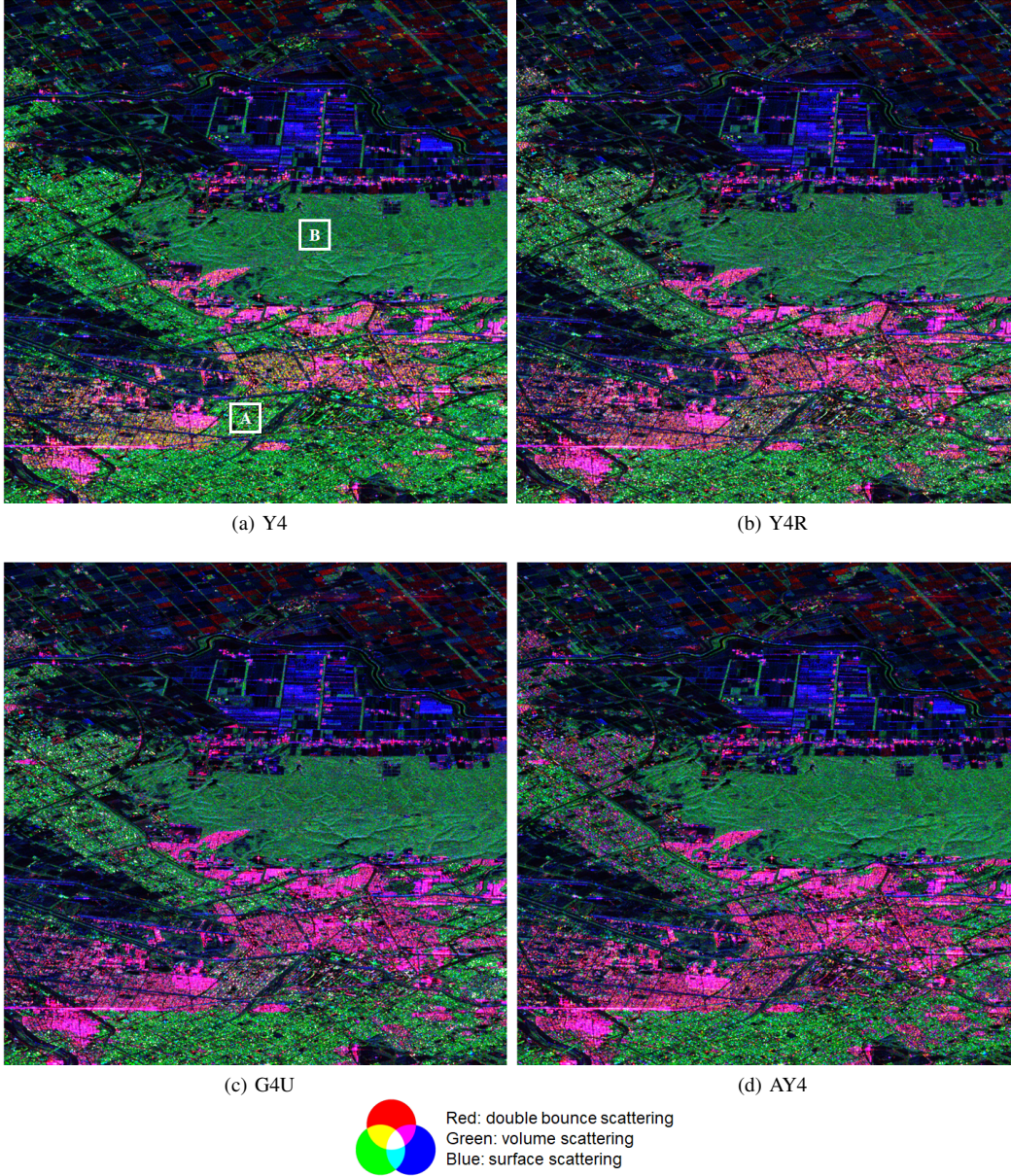


Fig. 5. Scattering mechanism interpretation result for Ebetsu area generated by (a) Y4, (b) Y4R, (c) G4U, and (d) AY4 which employs the proposed data arrangement.

STEP 2 For a certain pixel  $[I]$ , calculate its bias degree  $D_b^{[I]}$  in a  $N \times N$  window centered at  $[I]$  using equation (8).

IF  $|D_b^{[I]}| > \delta_b$  is true, go to STEP 3

IF  $|D_b^{[I]}| > \delta_b$  is false, go to STEP 5

STEP 3 Estimate the probability density function in the window centered at  $[I]$ , and determine the distributing center  $\mu^{[I]}$ , and the maximal density  $\Phi^{[I]}$  using equation (10) to (12).

IF  $|\mu^{[I]} - \mu_0| < \delta_\mu$  and  $\frac{|\Phi^{[I]} - \Phi_0|}{\Phi_0} < \delta_\Phi$  is true, go to STEP 4.

IF  $|\mu^{[I]} - \mu_0| < \delta_\mu$  and  $\frac{|\Phi^{[I]} - \Phi_0|}{\Phi_0} < \delta_\Phi$  is false, go to STEP 5.

STEP 4 Implement the rotation transformation for pixel  $[I]$  with  $\theta_0^{[I]}$  angle using equation (3).

STEP 5 Keep the pixel  $[I]$  as it is without rotation.

STEP 6 If the pixel is not the last pixel, move to the next pixel and go back to STEP 2. Otherwise, go to STEP 7.

STEP 7 Use the arranged data for further scattering mechanism interpretation.

#### D. Physical Meaning of the Arrangement

Basically, the arrangement with geometric rotation transformation calibrates the rotation shift about the radar line of sight. The direct factor causing such a shift is a target rotated from its standard local coordinate-system about the radar line of sight. In this rotation way, the angle shift in the received data is almost purely related to the target rotation angle  $\theta$ . However, such a rotation is rare in practical observation. For example, a building which can be seen as a rotated double

bounce reflection model about the radar line of sight must have an orientation rotation, and the ground must also have a certain slope at the same time. Usually, the target will simultaneously have rotations in other directions besides the rotation about the radar line of sight. In this case, many factors such as material feature, surface roughness, and detail structures on the facade will introduce obvious rotation shift to the received data. Moreover, the rotation shift can be also introduced by additional scattered wave generated in neighboring pixels. Different origins causing the rotation shift may coexist in a pixel. We cannot rigorously calibrate all the angle shifts by geometric rotation transformation. However, the arrangement forces the data to get close to the formation in the standard coordinate system.

#### IV. PERFORMANCE EVALUATION

The test data is the ALOS2-PALSAR2 level 1.1 fully polarimetric SAR data for Ebetsu area in Japan as shown in Fig. 4. The area includes  $3000 \times 3000$  pixels. The parameters used in the proposed data arrangement are  $N = 11$ ,  $\delta_b = 25\%$ ,  $\sigma_g = 0.08$ ,  $\delta_\mu = \frac{\pi}{36}$ , and  $\delta_\Phi = 50\%$ . The reference PDF is the Gaussian distribution with 99.7% possibility in the range  $\theta \in [-\pi/4, \pi/4]$  which has  $\mu_0 = 0$ , and  $\Phi_0 \approx 1.52$ . Note that, though this set of parameters is optimized for the ALOS-2 PALSAR2 data, it can be also used for other L band data with minor adjustment. Especially, if the resolution of a sensor is higher than ALOS2-PALSAR2, we suggest a higher  $\delta_b$ . If the resolution is lower, we suggest a lower  $\delta_b$ . The methods used in the comparison are : four-components decomposition (Y4), four-components decomposition with rotation of the averaged coherency matrix (Y4R), four-components decomposition with unitary transformation (G4U) , and Y4 using the data after the proposed single pixel based data arrangement (proposed AY4). The window size for speckle filtering used in Y4, Y4R and G4U is  $5 \times 5$ . The results are shown in Fig. 5. The results show that the method AY4 which employs the proposed algorithm have much more reddish pixels in man-made target area than other methods. It means that the double bounce scattering power contribution of the man-made target area in AY4 method is increased. Such an increasing makes the man-made targets more recognizable in further target identification. According to the discussions in section II, the rotation transformation may cause overestimation of double bounce and/or surface scattering power contribution in natural target areas. In order to evaluate the performance comprehensively, we should not focus only on the man-made target areas, we also need to test the scattering mechanism interpretation results in natural target areas.

A quantitative test of the scattering power contributions is done for the patch A and patch B shown in Fig. 5(a). The results are summarized in Table I. According to the results, the AY4 method provides the highest double bounce scattering power contribution (52.5%) in the city area (patch A). Whereas in the forest area (patch B), the AY4 method provides a highest volume scattering power contribution (52.0%) in comparison with Y4R and G4U. This value (52.0%) is very closed to the volume scattering power contribution provided by Y4 (52.9%)

TABLE I  
SCATTERING POWER CONTRIBUTIONS.

		Double Bounce	Volume	Surface	Helix
Patch A (city)	Y4	14.9%	51.3%	23.8%	10.0%
	Y4R	32.0%	28.6%	33.1%	6.3%
	G4U	32.7%	26.6%	34.3%	6.4%
	AY4	52.5%	13.2%	32.3%	2.0%
Patch B (forest)	Y4	10.4%	52.9%	29.7%	7.0%
	Y4R	13.1%	48.3%	31.6%	7.0%
	G4U	12.2%	48.2%	32.6%	7.0%
	AY4	10.8%	52.0%	30.2%	7.0%

which is a method without rotation transformation. The results show that, with the single pixel based rotation transformation, the proposed data arrangement has much higher performance in recognizing double bounce scattering in man-made target areas. Simultaneously, with the judgment on the orientation distributions of the configurations, the proposed algorithm avoids overestimating double bounce and/or surface scattering in natural target areas.

#### V. CONCLUSION

In this paper, we have proposed a data arrangement for fully polarimetric SAR. A quantitative test of the scattering power contributions for Ebetsu area observed by ALOS2-PALSAR2 has shown that the decomposition with the proposed coordinate-system arrangement provides the highest double bounce scattering power contribution in the city area, whereas, in the forest area, it provides a highest volume scattering power contribution in comparison with Y4R and G4U.

#### REFERENCES

- [1] S. R. Cloude and E. Pottier, "A review of target decomposition theorems in radar polarimetry," *IEEE Trans. Geosci. Remote Sens.*, vol. 34, pp. 498–518, 1996.
- [2] F. Shang and A. Hirose, "Averaged stokes vector based polarimetric sar data interpretation," *IEEE Trans. Geosci. Remote Sens.*, vol. 53, pp. 4536–4547, 2014.
- [3] A. Freeman and S. L. Durden, "A three-component scattering model for polarimetric SAR data," *IEEE Trans. Geosci. Remote Sens.*, vol. 36, pp. 963–973, 1998.
- [4] Y. Yamaguchi, T. Moriyama, M. Ishido, and H. Yamada, "Four-component scattering model for polarimetric SAR image decomposition," *IEEE Trans. Geosci. Remote Sens.*, vol. 43, pp. 1699–1706, 2005.
- [5] Y. Yamaguchi, A. Sato, W. M. Boerner, R. Sato, and H. Yamada, "Four-component scattering power decomposition with rotation of coherency matrix," *IEEE Trans. Geosci. Remote Sens.*, vol. 49, pp. 2251–2258, 2011.
- [6] G. Singh, Y. Yamaguchi, and S. E. Park, "General four-component scattering power decomposition with unitary transformation of coherency matrix," *IEEE Trans. Geosci. Remote Sens.*, vol. 51, pp. 3014–3022, 2013.
- [7] F. Shang and A. Hirose, "Use of coordinate rotation angle for improving PolSAR based man-made target detection," in *Int'l Symposium on Antennas and Propagation 2017*, 2017, p. 27.1272.
- [8] H. Kimura, "Radar polarization orientation shifts in built-up areas," *IEEE Geosci. Remote Sens. Lett.*, vol. 5, pp. 217–221, 2008.
- [9] J. S. Lee, D. L. Schuler, and T. L. Ainsworth, "Polarimetric SAR data compensation for terrain azimuth slope variation," *IEEE Trans. Geosci. Remote Sens.*, vol. 38, pp. 2153–2163, 2000.
- [10] S. Kidera, T. Sakamoto, and T. Sato, "Accurate uwb radar 3-d imaging algorithm for complex boundary without range points connections," *IEEE Trans. Geosci. Remote Sens.*, vol. 48, pp. 1993–2004, 2010.